



# I-CNN-LSTM: An Improved CNN-LSTM for Transient Stability Analysis of More Electric Aircraft Power Systems

Cong Gao<sup>1</sup> · Hongjuan Ge<sup>1</sup>

Received: 20 January 2024 / Accepted: 18 August 2024 / Published online: 8 September 2024  
© King Fahd University of Petroleum & Minerals 2024

## Abstract

High-power nonlinear load characteristics are one of the typical characteristics of multi-electric aircraft power systems. The study provides an improved CNN-LSTM stability analysis method for solving the stability problem of the aircraft power system caused by high-power nonlinear load switching. To address the issue of sample imbalance, this approach creatively incorporates the cost factor into the CNN loss function. In order to handle the issue of computational complexity, the projection layer is added to the LSTM, and a methodology known as CNN-LSTMP is proposed. This algorithm solves the problems of low computational efficiency and huge computational volume. The time series data utilized by the experiment are created by simulating the transient switching process. The data are then labeled, normalized, and model training is carried out. A deep learning algorithm that satisfies the prediction requirements can be created by applying this method to the established simulation model of a multi-electric aircraft power system for stability analysis. According to the results of the experiments, this method's transient stability analysis accuracy is 93.32%, which has a positive impact on transient analysis and may satisfy application requirements.

**Keywords** Transient stability analysis · Multi-electric aircraft power system · Improved CNN-LSTM algorithm · Time series analysis

## 1 Introduction

When it was first proposed in 1970s, the idea of a multi-electric aircraft (MEA) was known as an all-electric aircraft. The mechanical, electrical, hydraulic, and pneumatic subsystems are the four subsystems that MEA aims to replace with a single electrical system. Because MEA lowers fuel consumption, and the overall weight of the aircraft, and enhances the overall efficiency and dependability of the aviation system, it is frequently utilized. The primary functions of the airplane electrical system are power generation, conversion, and distribution. However, as a result of the system's high-power nonlinear load switching during this process, the stability of the aircraft power system becomes a more pressing concern. As a result, a significant area of research is now the stability analysis of electric aircraft power systems [1].

The Lyapunov function approach and its derivatives are currently the primary techniques for studying the transient stability of the power system of a multi-electric aircraft [2, 3]. In order to solve the conservatism issue raised by the conventional Lyapunov function method, literature [4] suggests a new adaptive Lyapunov function method that may estimate the critical clearing time with noticeably less conservatism. In order to determine the stability of big signals, literature [5] suggested a unified stability criterion based on the Liapunov linearization method; nevertheless, the model structure is complex and unsuitable for the analysis of complex power grids. Based on the conventional time-domain simulation method and the phase trajectory concavity of the time-domain simulation, Su Fu [6] and colleagues devised a rapid termination strategy for power system stability analysis. Literature [7] performs a system-level large-signal stability analysis of DC microgrids, creates an analogous model of sag-controlled DC microgrids, derives Lyapunov-based large-signal stability analysis and stability criteria, and uses bus voltage as an index to assess microgrid power stability. The issue that time-domain simulation (TDS) is too

✉ Hongjuan Ge  
gehongjuan1101a@nuaa.edu.cn

<sup>1</sup> College of Civil Aviation, Nanjing University of Aeronautics and Astronautics, Nanjing, China



dependent on solving nonlinear differential–algebraic equations of the power system is still challenging to resolve with this approach, though.

An other category of techniques for evaluating transient stability is grounded in the energy function, which evaluates stability by contrasting the system's critical energy and the transient energy during a disturbance [8–11]. Literature [10] leverages the measurement data acquired from the phase measurement unit (PMU) positioned at the generator bus to estimate the stability margins using the transient energy function (TEF) approach. This approach partially solves the issue of determining the equilibrium point of control instability in real-time applications; nonetheless, the approach necessitates precise system data, resulting in shortcomings in stability margin. ANTONIO et al. [12] presented the Brayton–Moser mixing potential combined with the Liapunov stability theorem for establishing the analytical estimates of the big signal stability bounds of the system. Comprehensive time-domain models of power system components were used to run extensive simulations. Practical estimates of these energies are challenging since some state variable observations are unavailable. It is challenging to adjust traditional transient stability evaluation techniques to shifting operating conditions and analytical requirements since they rely on offline time-domain simulations and energy functions.

Recent years have seen some excellent research outcomes based on pertinent algorithms for power system transient stability evaluation challenges, thanks to the development of machine learning algorithms. Literature [13] presented a core vector machine (CVM) to tackle the problem based on phasor measurement unit (PMU); the proposed technique has higher accuracy with least time consumption and space complexity. As a processing approach for high-dimensional data of the power system, Moulin et al. [14] suggested a learning-based nonlinear classifier that offers a useful solution to the dimensionality issue. A novel approach for the online evaluation of transient stability margins was presented in the literature [15]. It utilizes two-dimensional computer vision-based tidal current pictures (CVPFI) to extract topological information and pre-fault tidal characteristics. Next, under the expected contingency set, a complete convolutional neural network (CNN)-based network is built to map the link between steady-state currents and generator stability measures. In order to examine the stability of the rotor angle, literature [16] suggests supervised and unsupervised machine learning-based techniques. The efficacy of the proposed approaches is verified through the use of optimal tidal, steady state, and dynamic simulation tools. Deep trust network (DBN) is designed as a basis model for the offline training of deep learning models, which typically involves a large number of labeled samples and a time-consuming training process. This is another novel approach based on active

**Table 1** Comparison of power system stability analysis methods

Methods	Principles	Vantage	Disadvantages
Test method [2, 9]	Physical testing to verify system stability	High reliability by testing the system in a real environment	Costly to invest significant resources
Direct method [3–7]	Creates an energy function to explain power systems' transient stability	Offers a comparatively quick response time	Building the energy function is a difficulty
Time-domain simulation [8, 10–12]	Finds the precise dynamic behaviors of the system by solving the state-space differential equations	Excellent for the massive power systems	Largely dependent upon the model of the system Additional computational work is required
Artificial intelligence [13–17]	Applies various AI techniques to the evaluation of transient stability	Rapid analysis of data, excellent feature extraction capabilities	High computational costs and poor interpretability

migration learning that has been presented [17]. Because features in data-based transient stability analysis are frequently difficult to extract, numerous researchers have proposed a variety of techniques to address this problem, including the SIFT approach and the feature selection method using SHAP values. Nevertheless, the aforementioned techniques typically choose a large number of feature samples, leading to high-dimensional feature redundancy. Moreover, the sample imbalance issue—that is, the fact that unstable samples are significantly fewer than stable samples—as well as the challenge of the intricate computation of modeling associated with conventional stability analysis techniques are challenging to resolve. In order to facilitate a clearer comparison of the research techniques, we summarize the advantages and disadvantages of the four power system stability analysis methods in tabular form, as shown in Table 1.

This research presents an improved CNN-LSTMP transient stability analysis approach and conducts an extensive investigation of the problem from the characteristics of CNN

and LSTM algorithms to tackle the following concerns. The following succinctly describes the primary contributions of this paper's work:

*The first major contribution:* Projection layer is used for LSTM optimization and improvement. The issue of large-scale computation is effectively resolved, and the computational complexity is decreased to increase the effectiveness of transient stability analysis, by honing and optimizing LSTM with projection layers.

*Main contribution point 2:* Combined CNN-LSTMP approach for stability analysis: A solution integrating CNN and LSTMP algorithms for stability analysis has been devised to accurately handle the transient characteristics problem produced by high-power nonlinear load switching in multi-motor aviation power systems. This novel stability analysis method combines these two approaches, which can combine the characteristics of LSTMP in handling nonlinear time series with the advantages of CNN in feature extraction, and thus more effectively meets the demand for accuracy and efficiency in power system stability analysis.

*Main Contribution Point 3:* Introduction of the cost component as a creative solution to the sample imbalance problem in transitory data: The work embeds the cost element into the CNN loss function in a novel way. The method can improve the model's performance adaptability under different sample distributions, enhance the robustness of the model, and balance different sample categories. Thus, it makes the transient stability analysis of multi-electric aircraft power system more accurate.

The rest of the paper is organized as follows: Section 2 introduces the transient stability problem of a multi-electrical aircraft power system; Sect. 3 outlines the I-CNN-LSTM transient stability prediction method; Sect. 4 performs the experimental validation of the transient stability assessment method; and the conclusions are presented in Sect. 5.

## 2 Transient Stability Problems of Multi-electric Aircraft Power Systems

The multi-electric aircraft (MEA) power system, which is a hybrid HVAC and HVDC structure employed in the Boeing 787, is depicted in Fig. 1 of the research paper. Frequency-insensitive loads, such as the de-icing system and the base loads, are directly linked to the 230 V HVDC bus, which is supplied by a variable frequency generator. The 230 V primary bus is connected to the high-voltage DC bus using ATRU, and the electromechanical actuator used for flight control is connected to it through a pulse width modulation rectifier. The architecture maintains legacy 115V/400 Hz AC and 28 V DC power distribution converted from the HVDC bus utilizing a two-stage inverter power supply and transformer rectifier unit (TRU), respectively, to power a range

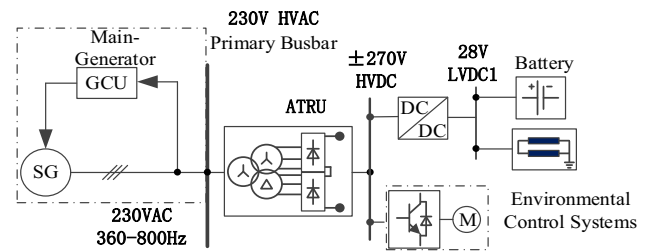


**Fig. 1** High-voltage DC power supply system with high-power nonlinear loads

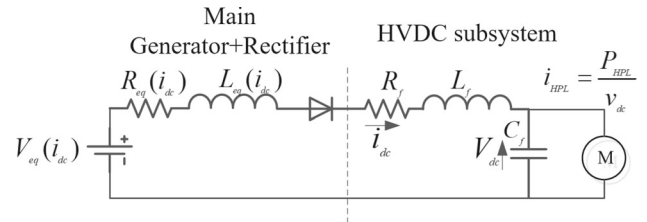


**Fig. 2** Simplified model of HVDC power system structure

of LVAC and LVDC legacy loads. Given the lengthy transmission lines influencing the distribution network, the line impedance between the SG and HVAC bus is another factor to be taken into consideration. Since different converters are used to link different loads to the distribution network, it is important to investigate the stability of the entire system to guarantee the MEA power system operates steadily. This includes taking into account how different subsystems interact as well as the unstable effects of capacitor banks.

After simplifying the system structure depicted in Fig. 2 for the high-voltage DC power supply system, it is required to analyze the stability of high-power nonlinear load switching.

The power supply consists of an ideal DC power supply  $V_{eq}$  and an equivalent internal resistance  $R_{eq}$ , with  $L_f$  and  $C_f$  being capacitors and inductors, respectively.  $P_{HPL}$  is a high-power load, which satisfies  $i_{HPL} = P_{HPL}/v_{dc}$ . The transition process of the closed-loop control system in the control of maintaining the output power constant is ignored. The steady-state equation can be determined as follows in light of the system structure depicted in Fig. 2:

$$\begin{cases} V_{dc} = V_{eq} - I_{HPL} R_{eq} \\ I_{HPL} = P_{HPL}/V_{dc} \end{cases} \quad (1)$$

where:  $V_{dc}$  and  $I_{HPL}$  are the load voltage and current,  $V_{eq}$  is the supply voltage,  $R_{eq}$  is the equivalent internal resistance, and  $P_{HPL}$  is the load power.

When high-power nonlinear load switching occurs at a node, the onboard power grid is affected by power fluctuations. The power borne by the network due to node power



fluctuations is:

$$\Delta P = |P_{HPL} - P_0| \quad (2)$$

The power impact of node power fluctuations on the entire system is:

$$\Delta P_A = \sum_{i=1}^{S_a} |P_{HPL} - P_0| \quad (3)$$

$\Delta P_A$  is the total power impact,  $P_0$  is the power before nonlinear large load switching,  $S_a$  is the set of all branches in the system.

In order to ensure that the system has a steady-state equilibrium operating point, the maximum power of the high-power load should be satisfied:

$$\Delta P_A \leq P_{\max} < \frac{V_s^2}{4R_{eq}} \quad (4)$$

According to the theory of hybrid potential function, the following conditions must be met by the system functioning at steady-state equilibrium in order for it to resume stable operation in the presence of a significant perturbation:

$$\frac{C_s}{L_s} > \frac{P_{HPL}}{V_{dc}^2 R_{eq}} \quad (5)$$

### 3 Proposed Methodology

#### 3.1 I-CNN-LSTM Algorithm

The input, convolutional layer, pooling layer, fully connected layer, and output layer make up the fundamental structure of a one-dimensional convolutional neural network (CNN), which is typically used to extract features from time series. The pooling layer and the convolutional layer are typically thought of as two separate layers that are arranged alternately, with one convolutional layer connected to the pooling layer, another convolutional layer to the pooling layer, and so on. A one-dimensional convolutional neural network is shown in Fig. 3.

The original graph  $X$  serves as the CNN's input. In this study, we refer to the convolutional layer  $H_i$  as the feature map of the  $i$ -th layer of the convolutional neural network ( $H_0 = X$ ). The generation method of  $H_i$  can be summarized as follows:

$$H_i = f(H_{i-1} \otimes W_i + b_i) \quad (6)$$

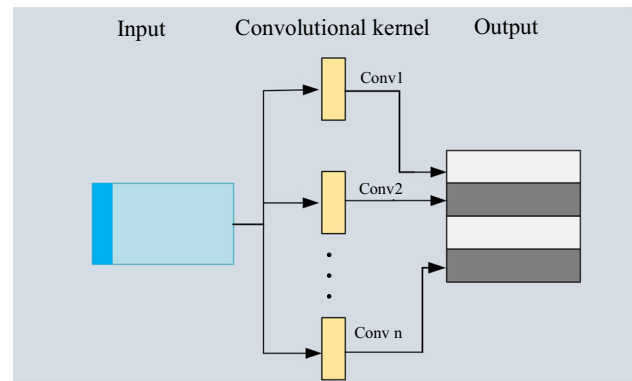


Fig. 3 One-dimensional convolutional neural network

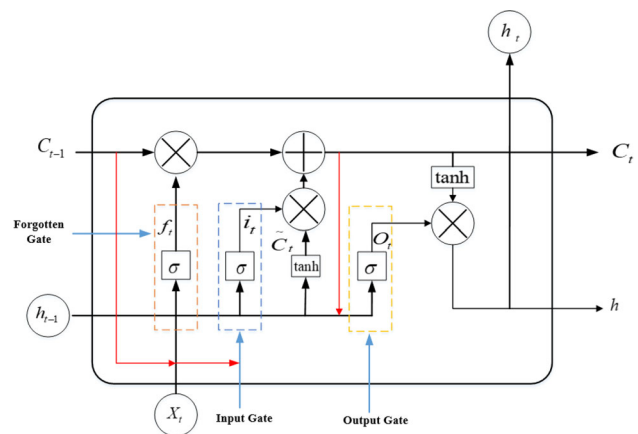


Fig. 4 Basic unit of LSTMP network

$W_i$  stands for the weight vector of the  $i$ -th layer convolutional kernel among them. The operational symbol " $\otimes$ " represents the convolution kernel and the  $i - 1$  layer feature map for convolution operation. The output of a convolution is added to the offset vector  $b_i$  of the  $i$ -th layer. Finally, the characteristic graph  $H_i$  of layer  $i$  is obtained through the nonlinear excitation function  $f(x)$ .

A temporal recurrent neural network called long-short term memory projection (LSTMP) was initially described in a research published in 1997. Because of its distinctive design, LSTMP is well suited for processing and forecasting significant events in time series with very long intervals and delays. For a given sequence  $(x_i, y_i)$ ,  $i = 1, \dots, N$ , where  $x_i = [x_{i1}, x_{i2}, \dots, x_{in}]^T \in R^N$ ,  $y_i = \{0, 1\}^N$ , the LSTMP model is shown in Fig. 4.

The memory blocks that make up the LSTMP architecture are a collection of cyclically connected subnets. Each block includes three multiplication cells, three outputs, an oblivion gate, and one or more self-connected memory cells. The state memory cell's oblivion component is determined by the input  $x_i$  of the oblivion gate, the state memory cell  $C_{t-1}$ , and the intermediate output  $h_{t-1}$ . In this research, we

perform LSTMP optimization and improvement, adding a projection layer, whose output serves as both historical data and an input for the subsequent layer [18]. The goal is to simplify the computation, and we further compress the output vector to decrease the cell unit. The computation method is expressed as follows:

$$i_t = \sigma(W_{xi}x_t + W_{hi}h_{t-1} + W_{ci}c_{t-1} + b_i) \quad (7)$$

$$f_t = \sigma(W_{xf}x_t + W_{hf}h_{t-1} + W_{cf}c_{t-1} + b_f) \quad (8)$$

$$\bar{C}_t = \phi(W_{\bar{c}x}x_t + W_{\bar{c}h}h_{t-1} + b_{\bar{c}}) \quad (9)$$

$$o_t = \sigma(W_{xo}x_t + W_{ho}h_{t-1} + W_{co}c_t + b_o) \quad (10)$$

$$h_t = \phi(C_t) \cdot o_t \quad (11)$$

$$r_t = W_{rm}h_t \quad (12)$$

where  $i_t, f_t, o_t, h_t, r_t$ , and  $C_t$  are input gates, forgetting gates, input nodes, output gates, intermediate outputs, and state units, respectively;  $W_{xi}, W_{hi}, W_{ci}, W_{xf}, W_{hf}, W_{cf}, W_{\bar{c}x}, W_{\bar{c}h}, W_{xo}, W_{ho}$ , and  $W_{co}$  are the corresponding gates with the coefficient matrix weights of the inputs  $x_t$  and the intermediate outputs  $h_{t-1}$ , respectively;  $b_i, b_f, b_{\bar{c}}$ , and  $b_o$  are the corresponding bias terms, respectively;  $\sigma$  is the change of the activation function; and  $\phi$  is the change of the tanh function.

Although LSTMP can handle nonlinear time series effectively, it nevertheless has the following two issues: (1) Parallel processing has a drawback, and its performance is subpar when compared to some of the newest networks. (2) Although LSTMP and its variants somewhat address the gradient problem of RNNs, this solution is still insufficient. Sequences of the order of 100 can be handled, but sequences of the order of 1000 or greater can be challenging. (3) It takes a long time to compute. Each LSTM cell implies four fully connected layers (MLPs), which can take some time if the network is extensive and the LSTM's time span is lengthy.

This study proposes enhancing the hybrid CNN-LSTM network model's structure because CNN can somewhat mitigate some of the LSTMP network's flaws. It combines the respective qualities of CNN and LSTM networks in its two primary components, comprising the input layer, convolutional layer, pooling layer, and output layer of the network structure. The convolutional layer and pooling layer construct a recurrent neural network, the output layer provides the prediction results, and the input layer performs the initial processing of the data to fulfill the criteria of the network input. In which, as shown in Fig. 5, the LSTM network is

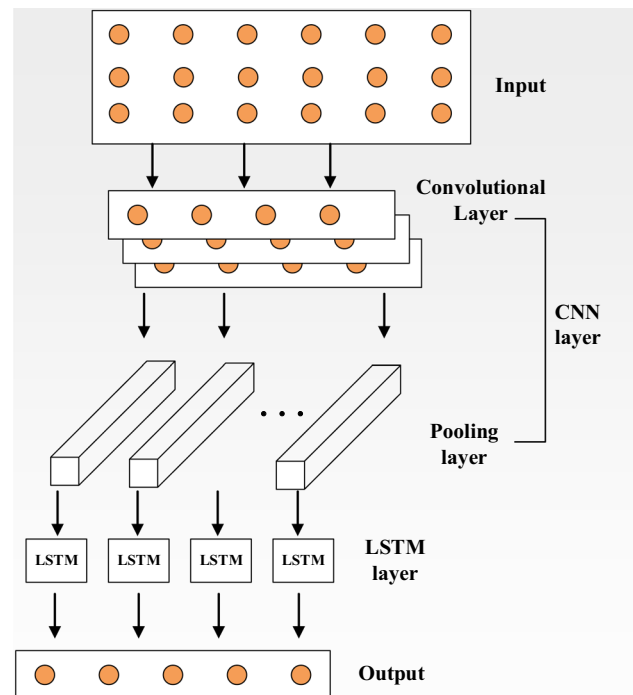


Fig. 5 Improved CNN-LSTM hybrid model structure

utilized for prediction while CNN is primarily employed for feature extraction.

Part 2 is used to segment the simulation data, and several time series data models are built. Each model can obtain the corresponding prediction results when the algorithm calls all the models for parallel learning after reading the first time series sample in the target domain. The performance of all models is then measured using root mean squared error, and the algorithm illustrates how the I-CNN-LSTM is implemented.

#### Algorithm .

**Input:** Training sample set time series data,  $(x_i, y_i)$ ,

$i = 1, \dots, N$ , where,  $x_i = [x_{i1}, x_{i2}, \dots, x_{in}]^T \in R^N$

$y_i = \{0, 1\}^N$

Parameters: M, Ld, Lr, Max

**Output:**  $y_i$

**Step:**

1: Based on part 2, extract and categorize the data to generate n samples of time series data,  $x_i, i = 1, \dots, N$ .

2: Classify the sample according to  $\eta = \frac{360^\circ - |\Delta\delta|_{\max}}{360^\circ + |\Delta\delta|_{\max}}$ .

3: If  $\eta > 0$ , then  $y_i = 1$ .

4: Import data and do data preprocessing

5: Set the parameters of the model and train it

6: Calculate RMSE

7: Calculate Acc according to (17)

**End**





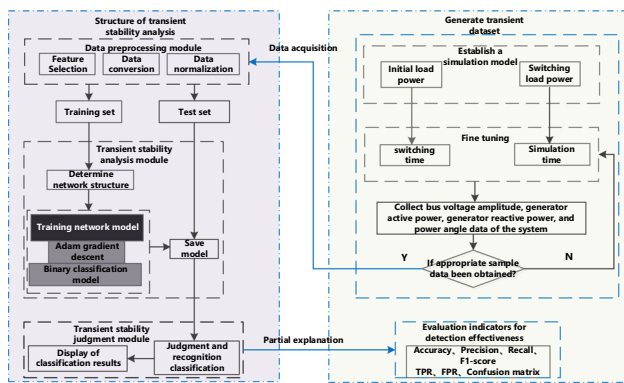


Fig. 6 Structure of transient stability analysis model

The transient stability analysis flow is depicted in Fig. 6. TSA based on time series data and deep learning involves three crucial phases: simulation modeling, dataset production, model development, and performance evaluation.

#### Remark1

1. Problem with long-term dependency: Long-term dependencies are challenging for traditional RNNs to capture because of the issues of gradient vanishing and gradient explosion when working with lengthy sequences. Additionally, by adding forgetting gates, input gates, and output gates to better capture long-term relationships in transient data sequences in transient stability analysis, LSTM can effectively overcome this problem.
2. Memory capacity: Long-term storage and updating of information is possible thanks to the larger memory capacity of LSTM. The performance of the model is impacted by the fact that traditional RNNs' simplistic structure makes it impossible for them to retain accurate information over an extended length of time.
3. Effectiveness in real-world applications: LSTM has demonstrated its effectiveness in a variety of real-world applications, including the analysis of time series data and natural language processing. Its tremendous modeling ability and practicality have been proven by its successful applications in machine translation, speech recognition, text generation, and other domains.

### 3.2 Transient Data Generation and Preprocessing

It is initially important to get historical data on the switching transient of high-power nonlinear loads in the power system to construct the initial prediction model. The choice of input features, as the initial step in the model creation, has a very significant impact on the prediction performance of the model, in addition to the excellent or bad prediction performance of the model, which is defined by the properties of the

model itself. Electrical quantities like bus voltage magnitude, generator active power, generator reactive power, rotational speed, rotor angular power imbalance, generator inertia time constant, FM coefficient, power injection, voltage magnitude, phase angle of each node, and other electrical quantities will fluctuate accordingly to varying degrees during the large load switching process of the aircraft power system. A significant amount of transient information is hidden in these electrical quantities.

The first stage in feature data selection is to choose electrical quantity data that can accurately capture the power system's transient characteristics. Second, in order to minimize data collecting time and accomplish quick transient stability prediction, easily measured data should be chosen. Furthermore, electrical quantities closely associated with transient stability should be chosen to minimize feature redundancy, minimize data demand, and prevent communication and model calculation delays brought on by an excessive amount of data. This recommendation is based on past research findings. This section suggests the following standards for choosing data kinds in light of the aforementioned arguments:

- (1) The data must be an electrical quantity that is simple to measure.
- (2) When applied as model output characteristics, this kind of data must have a strong correlation with transient stability as demonstrated by historical research, and its forecast accuracy is favorable.

According to the criteria, the input feature data can be chosen from the bus voltage magnitude, generator active power, generator reactive power, and generator power angle depending on the measurable data type knowable, correlation, and taking the power system stability theory into consideration. This study used SIMULINK to simulate a dynamic dataset at a sampling rate of 100 Hz for 0.2 s. The load level was adjusted to move from 30 to 60 KW to replicate the high-power nonlinear load switching state and generate enough samples. Following the high-power load switching, the operating data and electrical parameters of the power system were gathered. A total of 6000 sets of sample data were gathered, of which 4480 sets were classified as unstable samples that were required and 1520 sets as stable samples. In this instance, training data were used for 90% of the samples, and test data were used for the remaining 10%.

When using the I-CNN-LSTM algorithm, the selection of input variables must be carefully taken into account. Rotor angle and rotor speed are considered to be direct reflections of the system's transient stable condition per the definition of power system transient stability. As a result, their trajectories also provide extensive information regarding the system's transient stable state. However, compared to the generator

**Table 2** Input features used in the I-CNN-LSTM

Serial number	Input features
1	Active power per generator from $t$ to $3ftP$
2	Bus voltage amplitude from $t$ to $3ftU$
3	Generator power angle $t$ to $3ftV_g$
4	Generator reactive power from $t$ to $3ftQ$

voltage, electromagnetic power, and imbalanced power, their changes will take longer to occur due to the influence of system inertia and other factors. Utilizing the aforementioned analysis, the generator active power, bus voltage magnitude, power angle, and generator reactive power are chosen as inputs in this work, as indicated in Table 2.

Following a high-power nonlinear load switching, examples of typical variations in generator active power, bus voltage magnitude, generator rotor angle, and generator reactive power are shown in Fig. 7 for a multi-electric airplane power system. These waveforms were created by modeling load switching in an airplane power system with multiple electric motors. The transition causes a temporary unstable state that lasts for 0.1 s before recovering after 3 cycles.

Given a set of labels  $(x_i, y_i), i = 1, \dots, N$ , where  $x_i = [x_{i1}, x_{i2}, \dots, x_{in}]^T \in R^N, y_i = \{0, 1\}^N$ . In order to determine the stability state of each set of samples, the widely used transient stability criterion [19],  $\eta$  is used here as the transient stability index:

$$\eta = \frac{360^\circ - |\Delta\delta|_{\max}}{360^\circ + |\Delta\delta|_{\max}} \quad (13)$$

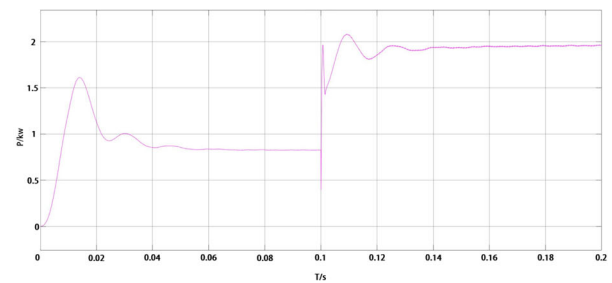
$$y_i = \begin{cases} 1, & \eta > 0 \\ 0, & \eta \leq 0 \end{cases} \quad (14)$$

In this case, it represents the greatest absolute value of the relative power angle between the generator and the exciter at a specific time throughout the simulation. A transitory stable sample exists if, and vice versa. It is a transient unstable sample that offers the information needed to train and test the transient stable model via labeling.

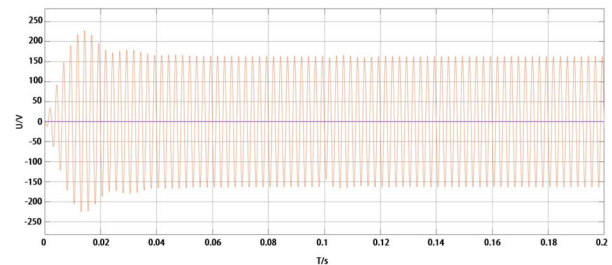
The interference brought on by distinct ranges of values for each parameter is lessened by normalizing the data to the same range. The equation, which in this study is in the range  $[0, 1]$ , normalizes all data.

$$x_{normal}^{i,j} = \frac{x^{i,j} - x_{\min}^j}{x_{\max}^j - x_{\min}^j} \quad (15)$$

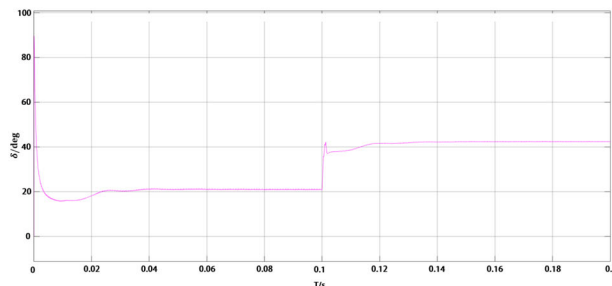
where  $x^{i,j}$  denotes the  $i$ -th data at the  $j$ -th moment;  $x_{\max}^j$  and  $x_{\min}^j$  denote the maximum and minimum values at the  $j$ -th moment, respectively;  $x_{normal}^{i,j}$  is the result of data normalization of  $x^{i,j}$ .



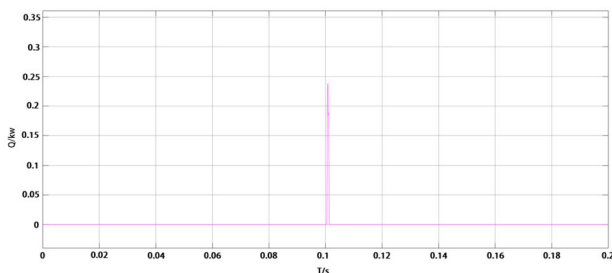
(a) Generator active power



(b) Bus voltage magnitude



(c) Generator power angle



(d) Generator reactive power

**Fig. 7** Changes of index parameters during switching of high-power loads

## 4 Validation of I-CNN-LSTM Transient Stability Assessment-based Method

The effectiveness of the proposed improved CNN-LSTM is tested using a multi-electric aircraft power system. The simulations were carried out using Mathworks' (USA) MATLAB/SIMULINK, a visual simulation program. The I-CNN-LSTM implementation and related data processing

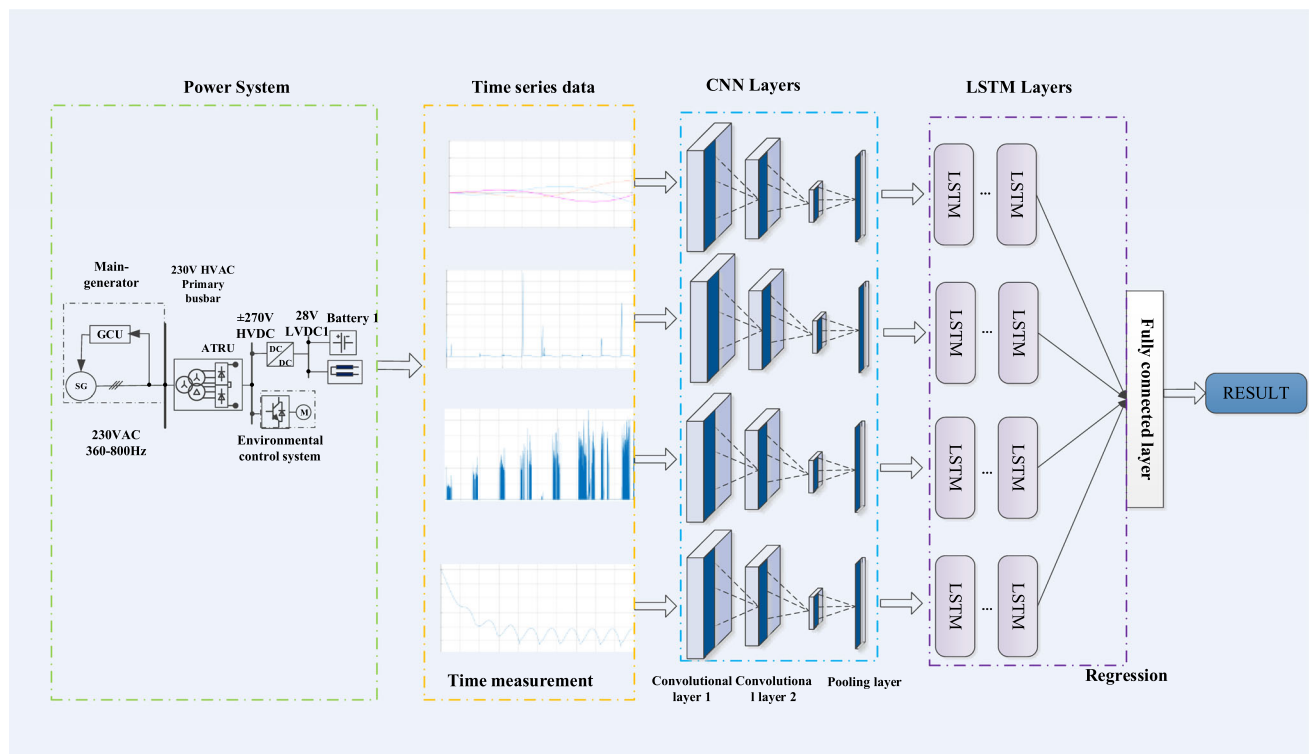


Fig. 8 Transient stability analysis framework based on improved CNN-LSTM

were carried out in MATLAB. The system's structure and hyperparameters are tuned in accordance with Table 1 for better I-CNN-LSTM learning.

#### 4.1 Multi-electric Aircraft Power Systems

Model the multi-electric aircraft power system in MATLAB/SIMULINK using a single generator. Using its extensive design resources, simulate the power system's operational flow.

Permanent magnet generator (PMG), exciter, and generator make up the majority of this model. The generator's input speed is 12,000 rpm, and an autotransformer rectifier (ATRU) transforms 235 V AC into 270 V DC so that it can power high-power nonlinear loads. The high-power load is switched in the simulation from 30 to 60KW, and during the switching process, the system's primary stability indicators are monitored.

#### 4.2 Algorithm Validation

The I-CNN-LSTM-based transient stability analysis framework for multiple electrical aircraft power systems that are proposed in this paper can be separated into steps, where the original data are processed by a normalization method based on the simulated images. Then, using the sliding time window approach and the predetermined time window size,

the normalized data are separated into various data sets. Finally, combining the benefits of CNN and LSTM, the I-CNN-LSTM basic model was created to obtain the initial identification results for various time window sizes. This model is represented schematically in Fig. 8.

##### 4.2.1 CNN, CNN-LSTM, and I-CNN-LSTM Algorithm Validation

For calculations and analysis, this section makes use of 600 test set samples and 5400 training set samples that were obtained through simulation on the multi-electric aircraft.

power system in Sect. 2. With current machine learning-based power system stability analysis techniques, compare and confirm. The objective function is gradually converged by altering the network weight parameters continually as the model is being trained, and L1 and L2 regularization factors are introduced, whereis the weight vector.

$$\|w\|_1 = \sum_{j=1}^m |w_j| \quad (16)$$

$$\|w\|_2^2 = \sum_{j=1}^m w_j^2 \quad (17)$$

The network layer and its accompanying parameter settings are displayed in Table 3 in accordance with the model



**Table 3** Model network parameter settings

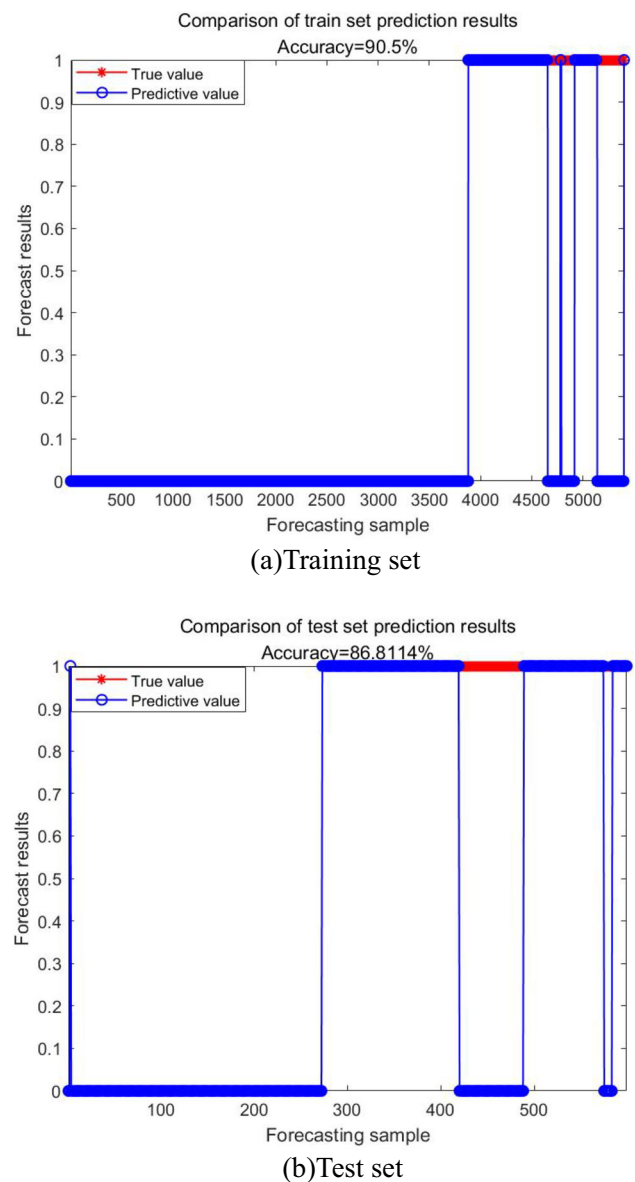
Parameter	Model		
	CNN	CNN-LSTM	Proposed Method
Max epochs	500	500	500
Initial learn rate	1e-3	1e-3	1e-3
Mini-batch size	600	600	600
L2Regularization	1e-4	1e-4	1e-4
Learn rate drop factor	0.2	0.2	0.2
Learn rate drop period	700	700	700
Train time	635 s	572 s	501 s

structure and data information. On a machine running Windows 10 with an Intel(R) Core(TM) i5-8265U CPU clocked at 1.60 GHz, an NVIDIA GeForce MX250 graphics card, and 16 GB of RAM, all experiments were carried out.

The training process for the models involves several key parameters: The maximum number of iterations is set to 500 to ensure comprehensive learning, the initial learning rate is 0.001 to balance convergence speed and stability, and the mini-batch size is 600 for optimal computational efficiency and performance. L2 regularization is applied with a coefficient of 0.0001 to prevent overfitting. The learning rate drop factor is 0.2, applied every 700 iterations, to fine-tune parameter adjustments and prevent oscillations. Training times are 635 s for CNN, 572 s for CNN-LSTM, and 501 s for the proposed method, indicating the proposed method's superior computational efficiency.

Adam's algorithm is the optimization algorithm utilized for training. In the training phase, 5400 samples were split into a training set and a test set in a 4:1 ratio. According to Fig. 9, when the quantity of training times grows, the model's accuracy keeps rising and its loss function keeps dropping. The test set is put up to test the model's generalizability and the model with the best accuracy rate. The test set will be kept track of throughout the training process and utilized to assess subsequent test samples.

The CNN model can achieve an accuracy of more than 90.50% on the training set and more than 86.81% on the test set after training, as demonstrated in Figs. 9 and 10. On the training set, the CNN-LSTM model can achieve an accuracy of 92.74%, and on the test set, it can achieve more than 91.15%. From Fig. 11, it can be concluded that the accuracy of the I-CNN-LSTM model on the training set exceeds 95.74%, and the accuracy on the validation set exceeds 93.32%. It is clear that the CNN and CNN-LSTM models have poor generalization abilities for samples that have not taken part in training, but the I-CNN-LSTM model exhibits the model's strong assessment capabilities for such data. Figure 12 displays each model's training and testing sets' accuracy.

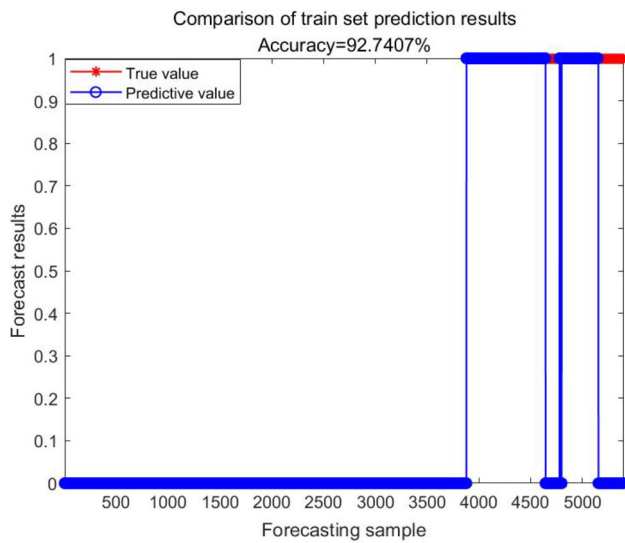
**Fig. 9** Accuracy of CNN model training set and test set

The characteristics of sample imbalance prevent the accuracy rate and error rate indicators from accurately evaluating the model generalization abilities because the number of samples in each category is not equal in the actual dataset. In this study, a confusion matrix is utilized to quantitatively assess the model's performance, describing the generalizability of the model from four perspectives: accuracy, precision, recall, and  $F1$ -score. Table 4 also displays the confusion matrix for transient stability assessment.

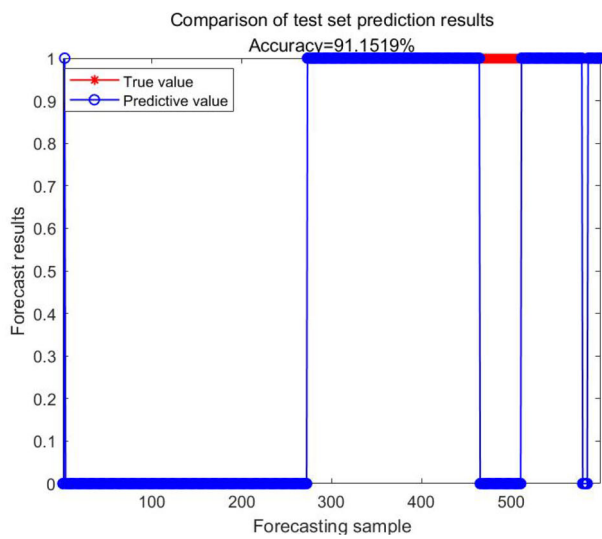
The calculation formulas for accuracy, precision, recall, and  $F1$  score are as follows:

$$Acc = \frac{TP + TN}{TP + FP + FN + TN} \quad (18)$$





(a) Training set



(b) Test set

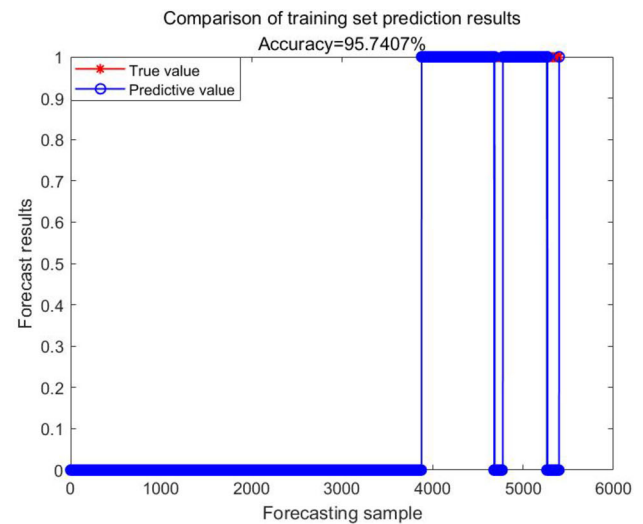
**Fig. 10** Accuracy of CNN-LSTM model training set and test set

$$Pre = \frac{TP}{TP + FP} \quad (19)$$

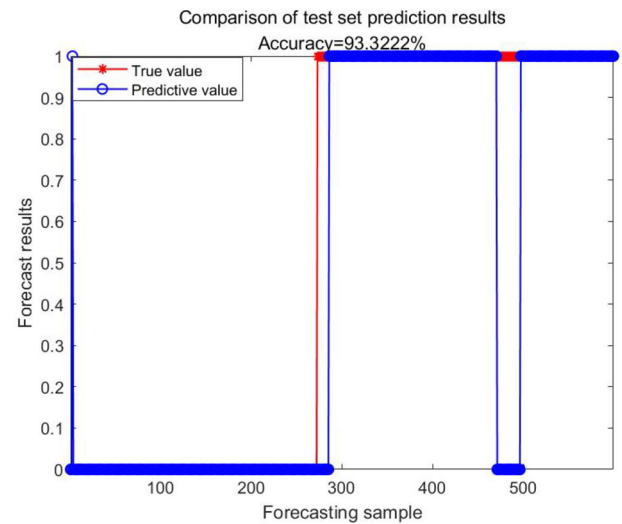
$$Recall = \frac{TP}{TP + FN} \quad (20)$$

$$F1 - score = \frac{2 \times Prec \times Recall}{Prec + Recall} \quad (21)$$

As shown in Figs. 13, 14, and 15, this research employs a confusion matrix to illustrate the evaluation criteria and model performance.



(a) Training set



(b) Test set

**Fig. 11** Proposed method model training set and test set accuracies

#### 4.2.2 Comparative Analysis of Models

A comparative bar chart is used to assess the performance of several models in power system transient stability prediction in terms of accuracy (Acc), precision (Pre), recall, and F1-score to illustrate each model's performance better. Bar charts representing the metrics of SVM, KNN, CNN, CNN-LSTM, incremental learning, deep residual shrinkage network (DRSN), and

the suggested approach are displayed in Fig. 16.

A detailed analysis is conducted on each model's experimental results and their implications. Table 5 displays the evaluation findings, including accuracy (Acc), precision

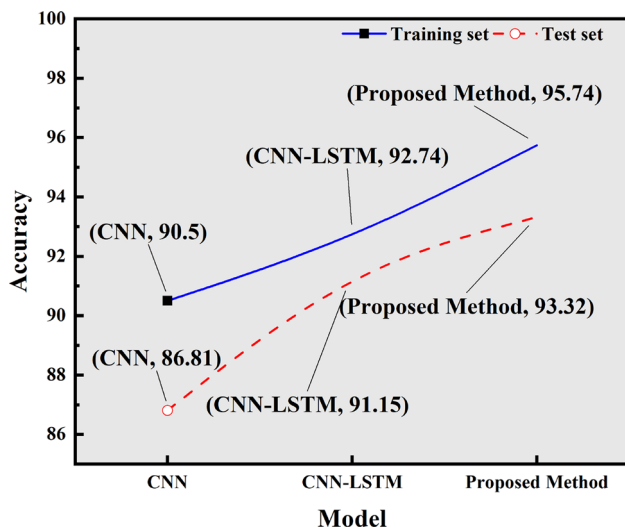


**Fig. 12** Comparison of the accuracy of the training and test sets of each model

**Table 4** Confusion matrix classification results

Projected results	Truthful labeling	
	Transient stabilization	Transient instability
Transient stabilization ( $i = 0$ )	TP	FP
Transient destabilization ( $i = 1$ )	FN	TN

(Pre), recall, and  $F1$ -score, of the various models used to predict power system transient stability.

SVM performs well in detecting positive samples, as evidenced by its pre of 91.41%, but its recall is quite low, suggesting that more positive samples may go unidentified. Better  $F1$  and accuracy scores show that SVM does a good job of balancing precision and recall. With higher  $F1$  scores, KNN outperforms in pre and recall but has a lower overall accuracy of 86.11%. This could be because KNN performs less well with high-dimensional feature space. While incremental learning is effective at real-time adaptation to new data, it may face difficulties when the distribution of data undergoes major changes. With a higher  $F1$  score of 91.41%, the performance in handling dynamic data is more balanced. By adding a soft threshold function, DRSN effectively suppresses noise and enhances the model's accuracy and stability. Its excellent pre (98.76%) and recall (86.38%) ratings suggest that it is still quite effective in loud settings. CNN's high-precision rate (99.60%) suggests that it is capable of extracting features, but its low recall leads to a low

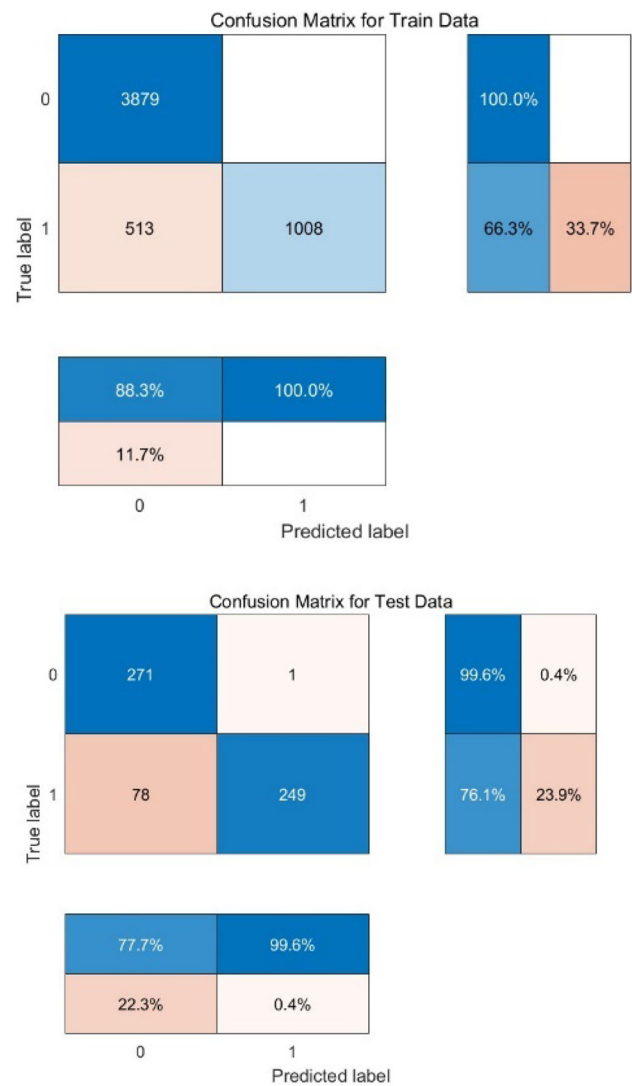


**Fig. 13** CNN confusion matrix

$F1$  score overall. This suggests that CNN's ability to handle temporal elements is lacking. The CNN-LSTM approach combines the temporal modeling capability of LSTM with the feature extraction capability of CNN. It performs better overall, though not as well as the suggested method.

This study presents the I-CNN-LSTM method, which outperforms all other methods in terms of metrics, particularly accuracy (93.32%) and  $F1$  (92.90%). This is because the technique seamlessly integrates integrated feature extraction and temporal modeling capabilities with the benefits of both CNN and LSTM. The suggested approach is very applicable in real-world scenarios, particularly when predicting power system stability, which calls for real-time analysis and great precision.



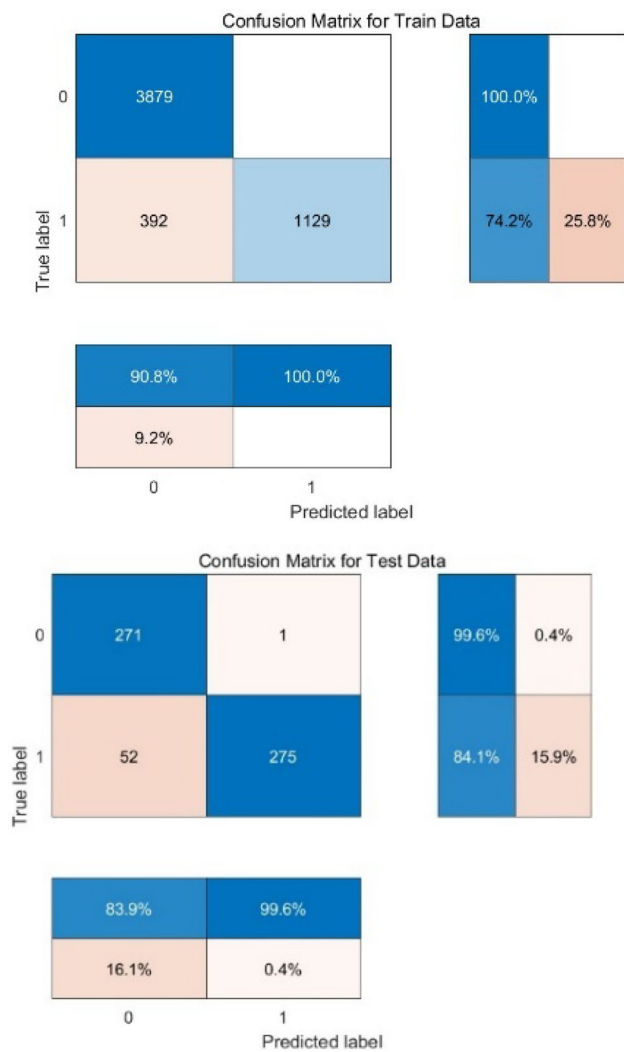


Fig. 14 CNN-LSTM confusion matrix

## 5 Conclusion

This paper's research provides an accurate and quick I-CNN-LSTM approach using transient stability data. The method addresses the issue that standard transient stability methods have because of their high computational complexity and difficulty in conducting accurate and timely analyses. With guaranteed precision, it assesses the multi-electric aircraft power system's transient stability following a significant load switch. This paper proposes the I-CNN-LSTM transient stability analysis approach, which better accomplishes the transient stability analysis of power systems by providing a thorough portrayal of the time series data and a partial synthesis of the global and local features. The contributions of our work include three aspects:

1. Improved transient stability prediction accuracy: Through high-precision prediction performance, the



Fig. 15 Proposed method confusion matrix

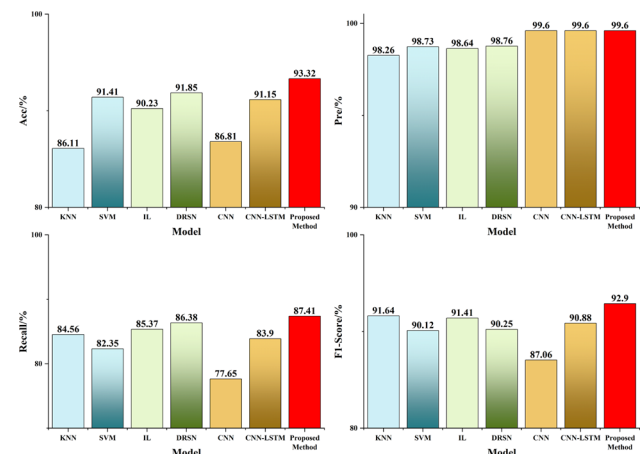


Fig. 16 Comparison of the main evaluation indicators for each model

**Table 5** Comparison of transient stability prediction evaluation results

Model	Acc/%	Pre/%	Recall/%	F1-score/%
SVM	91.41	98.73	82.35	90.12
KNN	86.11	98.26	84.56	91.64
IL	90.23	98.64	85.37	91.41
DRSN	91.85	98.76	86.38	90.25
CNN	86.81	99.60	77.65	87.06
CNN-LSTM	91.15	99.60	83.90	90.88
Proposed method	93.32	99.60	87.41	92.90

proposed I-CNN-LSTM method greatly increases the accuracy of transient stability analysis. I-CNN-LSTM does well in several evaluation metrics compared to other deep learning algorithms and conventional methods.

2. More quick computation: Despite traditional transient stability analysis approaches, which frequently call for intricate modeling and a significant investment in processing power, the I-CNN-LSTM approach uses deep learning techniques to streamline the computational process and enable quick analysis with absolute accuracy.
3. Encouraging the creation of the aviation smart grid: An essential component of the aircraft smart grid is an effective transient stability prediction approach. Through improved preventive maintenance and management, enhanced system stability, and improved adaptability to the complex grid environment, the power system can benefit from applying the I-CNN-LSTM approach.

Research limitations and prospective avenues for investigation: Real-time and accurate data, the model's robustness, and its interpretability are issues that need to be further addressed in actual implementations. Subsequent studies may concentrate on improving the model's interpretability and robustness in real-world scenarios. A network with a larger scale would be tested to verify the scalability of the proposed method.

**Acknowledgements** This work was supported by the National Natural Science Foundation of China (Grant U2233205 and U2133203).

**Author Contributions** H.G. designed the study. C.G. performed numerical experiments, performed data analysis, and wrote the paper. All the authors discussed the results and commented on the manuscript.

**Data Availability** The datasets generated and analyzed during the current study are not publicly available due to time limitations but are available from the corresponding author on reasonable request.

## Declarations

**Competing interests** The authors declare no competing interests.

## References

1. Zhang, Z.R. et al.: *Inverter AC Power Supply System for Multi-electric Aircraft*. Science Press. 36–47 (2022).
2. Taul, M.G.; Davari, P.; Blaabjerg, F.: An overview of assessment methods for synchronization stability of grid-connected converters under severe symmetrical grid faults. *IEEE Trans. Power. Electr.* **34**(10), 9655–9670 (2019). <https://doi.org/10.1109/TPEL.2019.2892142>
3. Inbar, S.; Nir, S.: Spectral analysis of a non-equilibrium stochastic dynamics on a general network. *Sci. Rep.* **8**(1), 14333 (2018). <https://doi.org/10.1038/s41598-018-32650-5>
4. Zhang, Y.; Zhang, C.; Cai, X.: Large-signal grid-synchronization stability analysis of pll-based vscs using lyapunov's direct method. *IEEE T. Power. Syst.* **37**(1), 788–791 (2022). <https://doi.org/10.1109/TPWRS.2021.3089025>
5. Qiu, Z.T.; Duan, C.; Yao, W., et al.: Adaptive lyapunov function method for power system transient stability analysis. *IEEE T Power Syst.* **38**(4), 3331–33449 (2023). <https://doi.org/10.1109/TPWRS.2022.3199448>
6. Su, F.; Yang, S.H.; Wang, H.Y., et al.: Research on fast termination algorithm for transient stability time domain simulation of power systems. *Chin J Elect Eng* **37**(15), 4372–4378 (2017)
7. Che, Y.B.; Xu, J.M.; Shi, K., et al.: Stability analysis of aircraft power systems based on a unified large signal model. *Energies* **10**(11), 1739 (2017). <https://doi.org/10.3390/en1011739>
8. Xue, Y.C.; Zhang, Z.R.; Zhang, N., et al.: Transient stability analysis and enhancement control strategies for interconnected AC systems with VSC-Based generations. *INT. J. Elec. Power.* **149**, 109017 (2023). <https://doi.org/10.1016/j.ijepes.2023.109017>
9. Xie, W.Q.; Han, M.X.; Cao, W.Y., et al.: System-level large-signal stability analysis of droop-controlled dc microgrids. *IEEE T. Power. Elec.* **36**(4), 4224–4236 (2021). <https://doi.org/10.1109/TPEL.2020.3019311>
10. Bhui, P.; Senroy, N.: Real-time prediction and control of transient stability using transient energy function. *IEEE T. Power. Syst.* **32**(2), 923–934 (2017). <https://doi.org/10.1109/TPWRS.2016.2564444>
11. Al-Fahoum, A.; Ghobon, T.: An applied approach for speed estimation of induction motors using sensorless flux observer system with sliding mode field oriented control. *IJEET* **11**(6), 109–122 (2020). <https://doi.org/10.34218/IJEET.11.6.2020.011>
12. Antonio, G.; Wang, J.B.: Large signal stability analysis of "more electric" aircraft power systems with constant power loads. *IEEE T. Aero. Elec Sys.* **48**(1), 477–489 (2012). <https://doi.org/10.1109/TAES.2012.6129649>
13. Wang, B.; Fang, B.W.; Wang, Y.J., et al.: Power system transient stability assessment based on big data and the core vector machine. *IEEE T Smart Grid.* **7**(5), 2561–2570 (2016). <https://doi.org/10.1109/TSG.2016.2549063>





14. Moulin, L.S.; Alves da Silva, A.P.; El-Sharkawi, M.A.: Support vector machines for transient stability analysis of large-scale power systems. *IEEE T. Power. Syst.* **19**(2), 818–825 (2004). <https://doi.org/10.1109/TPWRS.2004.826018>
15. Shi, Z.T.; Yao, W.; Tang, Y., et al.: Intelligent power system stability assessment and dominant instability mode identification using integrated active deep learning. *IEEE T Neur Net Lear* (2023). <https://doi.org/10.1109/TNNLS.2023.3238168>
16. Tayeb, M.; Geza, J.; Jose, R.: A power system stability assessment framework using machine-learning. *Electr. Power Syst. Res.* **216**, 108981 (2023). <https://doi.org/10.1016/j.epsr.2022.108981>
17. Gomez, F.R.; Rajapakse, A.D.; Annakkage, U.D.: Support vector machine-based algorithm for post-fault transient stability status prediction using synchronized measurements. *IEEE T. Power. Syst.* **26**(3), 1474–1483 (2011). <https://doi.org/10.1109/TPWRS.2010.2082575>
18. Klaus, G.; Rupesh, K.; Srivastava, J.K., et al.: LSTM: A Search Space Odyssey. *IEEE T Neur Net Lear.* **28**(10), 2222–2232 (2017). <https://doi.org/10.1109/TNNLS.2016.2582924>
19. Francisco, R.G.; Athula, D.; Udaya, D.A., et al.: Support Vector Machine-Based Algorithm for Post-Fault Transient Stability Status Prediction Using Synchronized Measurements. *IEEE T. Power. Syst.* **26**(3), 1474–1483 (2011). <https://doi.org/10.1109/TPWRS.2010.2082575>

Springer Nature or its licensor (e.g. a society or other partner) holds exclusive rights to this article under a publishing agreement with the author(s) or other rightsholder(s); author self-archiving of the accepted manuscript version of this article is solely governed by the terms of such publishing agreement and applicable law.